ARTICLE

Ultrasonic-Assisted Nanodimensional Self-Assembly of Poly-3-hexylthiophene for Organic Photovoltaic Cells

Bong-Gi Kim,[†] Myung-Su Kim,[‡,⊥] and Jinsang Kim[†,‡,§,*]

[†]Macromolecular Science and Engineering, [‡]Department of Materials Science and Engineering, and [§]Chemical Engineering, University of Michigan, Ann Arbor, Michigan 48109. [⊥]Current address: Solar Cell Division, Samsung Electronics, Giheunggu, Yonginsi, Gyounggido, South Korea.

ABSTRACT We have demonstrated ultrasonic-assisted nanodimensional self-assembly of a conjugated polymer, P3HT, depending on its regioregularity, on solvent polarity, and on light irradiation. The resulting P3HT nanowires were investigated by means of AFM, UV—vis, and XRD and compared with films made by a conventional thermal annealing method. Obtained results indicate that ultrasonic agitation effectively generates P3HT nanowires, exemplifying a quick route to nanoscale morphology control which contributes to better organic photovoltaic cell performance.

KEYWORDS: self-assembly · photovoltaic devices · conjugated polymers · nanowires · organic electronics

In the past few years, organic photovoltaic cells (OPVCs), especially based on the poly-3-hexylthiophene (P3HT)/[6,6]-phenyl C_{61}-butyric acid methyl ester ($PC_{61}BM$) blend system, have drawn much interest as a promising, cost-effective alternative to silicon-based solar cells. The power conversion efficiency (PCE) of P3HT/PCBM blend solar cells including tandem cells has improved rapidly and is currently in the range of 3.5−6.5%.[1−5] Morphological studies of the P3HT/PCBM system by means of atomic force microscopy (AFM), X-ray diffraction (XRD), and transmission electron microscopy (TEM) imply that enhanced crystallization of P3HT in the blend film plays a critical role in improving PCE. Accordingly, several methods have been developed to increase the crystallinity of P3HT including thermal treatment,[2] solvent-assisted annealing,[3] and additive-assisted annealing.[6] In addition, fully aggregated P3HT fibers, isolated from concentrated solution, have been used to enhance the molecular packing of P3HT.[7,8] However, understanding and controlling optimum morphological condition of the P3HT/PCBM blend system for better device performance has not been fully established.

Recently, several research groups found that P3HT could form aggregates spontaneously in a solution when the polymer was treated with an unfriendly solvent.[9−11] However, even though the absorption coefficient was dramatically increased, the photovoltaic device made of the preaggregated P3HT showed poorer performance than or, at best, similar performance to the device with a thermally induced aggregated P3HT/PCBM blend.[12] We believe that the low efficiency is likely due to the domain size of the preaggregated P3HT that is beyond the critical exciton diffusion length.

In this contribution, we investigate several important parameters to realize homogeneous P3HT nanowire (NW) formation in an organic solvent system and to control the domain size to achieve highly efficient photovoltaic devices. Ultrasonic irradiation has often been utilized to nucleate and grow molecular crystals.[13,14] However, ultrasonic irradiation seldom favors the formation of an ordered assembly,[15] particularly for polymeric materials, because of their low crystallinity.

RESULTS AND DISCUSSION

P3HT Nanowire Preparation. We found that applying ultrasonic waves to a P3HT solution containing a dipolar solvent, such as acetonitrile (AN), could facilitate P3HT aggregation to form an aggregate (video in Supporting Information) that can be spin-cast easily with PCBM. As shown in Scheme 1, nonpolar P3HT is initially completely solvated by nonpolar good solvents, such as chlorobenzene (CB). As the solvent polarity increases by means of adding a polar solvent, the interaction between P3HT and the solvent becomes weaker while the interac-

*Address correspondence to jinsang@umich.edu.

Received for review November 5, 2009 and accepted February 24, 2010.

Published online March 2, 2010. 10.1021/nn901568w

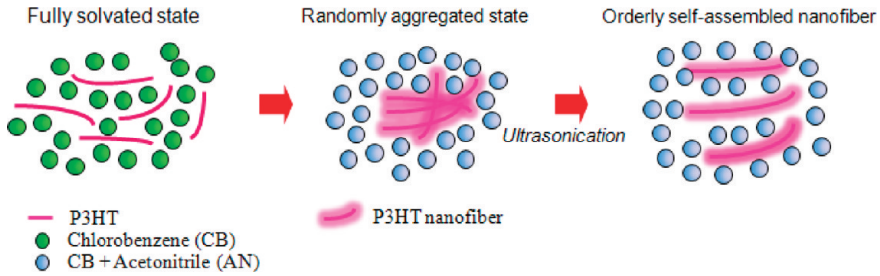

Scheme 1. Schematic illustration of P3HT aggregation in a solvent system containing a dipolar solvent.

tion among P3HT polymer chains becomes dominant, putting P3HT into a randomly aggregated state. However, the aggregation kinetics are slow, leading to a low degree of crystallization; the low mobility of the randomly aggregated P3HT only allows for the formation of randomly entangled polymer chains. We applied ultrasonic irradiation to disassemble the P3HT chains from the randomly aggregated state. As soon as P3HT chains are separated apart by the ultrasonic irradiation, they want to aggregate again because of the unfavorable interaction with the polar enough solvent system. Fast and multiple cycles of the aggregation and deaggregation processes induce ordered P3HT aggregation. Obtained P3HT aggregate was characterized and compared with bulk P3HT solution. The aggregation-induced color change from orange to dark purple is a well-known phenomenon of P3HT.[3,4] Therefore, the degree of aggregation of P3HT can be examined by analyzing the color change, as shown in Figure 1. While the 98% regioregular P3HT solution was dark purple after ultrasonic treatment for 2 min, 91% regioregular polymer developed lighter purple color. When ultrasonic treatment was not applied, the 91 and 98% regioregular P3HT solutions did not show the color development within the applied time period. Regioregular P3HT having the lower regularity also showed slow crystallization kinetics and low crystallinity upon thermal annealing because the low regularity hinders effective interchain stacking of P3HT .[4] As shown in Figure 2, ultrasonication produces a P3HT nanowire having a uniform width of 20−25 nm, while bulk P3HT solution does not show any aggregated feature.

To investigate the effect of a dipolar solvent on the aggregation behavior of P3HT, we examined several solvents having various polarity.[16] Nonpolar hexane, which is a poor solvent to P3HT, was also included in the study to see whether the solubility itself had the dominant effect on the aggregation phenomenon of P3HT. In this investigation, we used only 91% regioregular P3HT to confirm the solvent effect on aggregation because 98% regioregular P3HT may not exhibit a distinct difference due to its very fast aggregation behavior. Ten milligrams of P3HT was dissolved in 1 mL of cosolvent composed of 90 vol % of chlorobenzene and 10 vol % of a dipolar solvent. After ultrasonic treatment for 2 min, samples were stored under ambient light and under a dark condition for 2 h, respectively. Regarding the samples kept under ambient light, the aggregation behavior of P3HT was enhanced as solvent polarity increased, judging from their color change, as illustrated in Figure S1 (Supporting Information). Nonpolar hexane did not cause any noticeable color change even though it is a poor solvent to P3HT, implying that solubility itself is not a critical factor for the aggregation behavior. Interestingly, the samples kept under room light showed faster aggregation propensity than the same samples kept under a dark condition. Planarization of the P3HT backbone induced by photoexcitation[17] likely accelerates the molecular aggregation. The obtained P3HT nanowires were stable, unable to be dis-

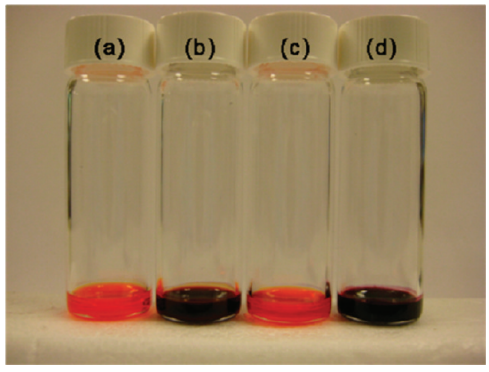

Figure 1. Aggregation behavior of P3HT in chlorobenzene containing 5 vol % of acetonitrile, (a) 91% regioregular P3HT without ultrasonication, (b) 91% regioregular P3HT with ultrasonication, (c) 98% regioregular P3HT without ultrasonication, and (d) 98% regioregular P3HT with ultrasonication. The image was taken 2 h after applying ultrasonication for 2 min.

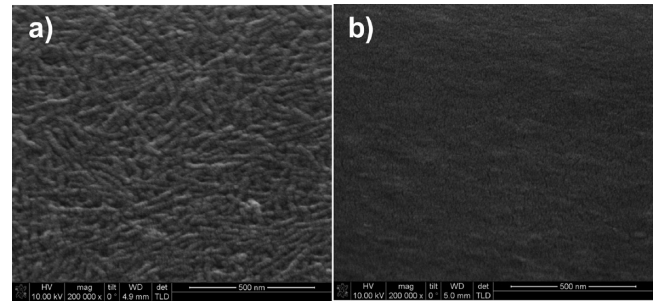

Figure 2. SEM images of (a) P3HT nanowires prepared by the ultrasonic-assisted self-assembly method (10 mg of P3HT in 1 mL of chlorobenzene (95 vol %)/acetonitrile(5 vol %) cosolvent) and (b) bulk P3HT solution (10 mg of P3HT in 1 mL of chlorobenzene). All images were taken using 98% regioregular P3HT, and films were not thermally treated after spin-casting. Scale bar is 500 nm.

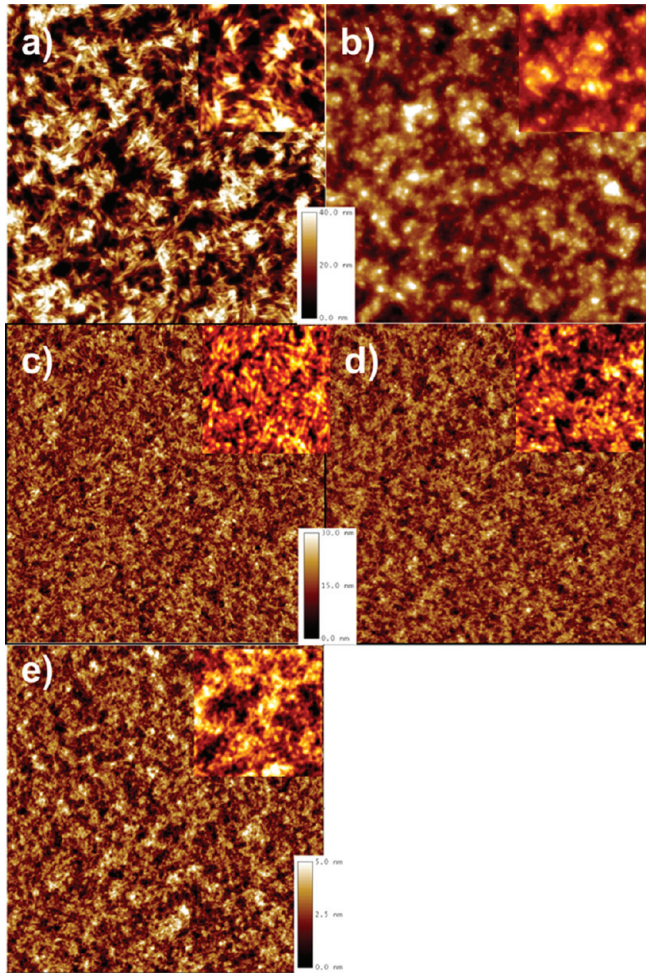

Figure 3. Tapping mode AFM images of P3HT NW/$PC_{61}BM$ films. The scan area is 5 μm × 5 μm, and the insets are magnified areas of 1 μm × 1 μm: (a,b) 91% RR P3HT NW/$PC_{61}BM$ blend before and after thermal annealing, (c,d) 98% RR P3HT NW/$PC_{61}BM$ blend film before and after thermal annealing, and (e) 98% RR P3HT/PCBM blend film after thermal annealing.

sembled by additional ultrasonication at ambient temperature. However, if the suspension of the P3HT nanowires was heated at 60 °C, the nanowires disassembled and the suspension became an orange solution. Among the solvents we tested, acetonitrile most efficiently promoted the P3HT aggregation. We could obtain homogeneous P3HT suspensions from limited volume ranges of acetonitrile to chlorobenzene (5−15 vol % for 91% RR P3HT and 3−10 vol % for 98% RR P3HT), and the conversion yields to NWs (67 and 88% for 91% RR P3HT and 98% RR P3HT, respectively) were calculated after directly collecting NWs using syringe filters (pore size ~ 450 nm) when acetonitrile was used as dipolar solvent. The resulting suspensions were spin-cast after blending with $PC_{61}BM$ at room temperature to form a thin layer film for further investigation.

Blend Film Morphology. We investigated the features of the P3HT nanowires by examining the spin-cast film morphology with AFM and SEM. As shown in Figure 3a,c and Figure 4b,c, we consistently observed P3HT nanowires having a relatively uniform width of 40−50 nm with similar shape, as seen in Figure 2a. The bright regions are P3HT-rich nanowires, and the dark regions are $PC_{61}BM$-rich amorphous regions.[2,7,12] This nanowire morphology is different from the featureless surface observed in the films of conventional P3HT/PC_{61}MB blend solutions (Figure 3e). The film prepared from the 91% RR P3HT NW/$PC_{61}BM$ blend showed larger size nanowires than that of the 98% RR P3HT NW/$PC_{61}BM$ blend. That is likely because 91% RR P3HT forms nanowires of lower crystallinity and exhibit looser phase separation between crystals and amorphous P3HT/$PC_{61}BM$. Thermal annealing at 150 °C for 15 min was applied to the film, and while the 98% RR P3HT NW/$PC_{61}BM$ film did not show any noticeable changes, the image contrast of the 91% RR P3HT NW/$PC_{61}BM$ film significantly diminished. We think that the difference came from the different amount of amorphous P3HT regions that were not involved in the P3HT NW but form the tie region between the P3HT NWs. The amorphous P3HT distributed around the P3HT nanowires likely forms a smoother layer by filling the clefts between the nanowires during the thermal annealing. Thermal annealing will induce further crystal packing and phase segregation and therefore may explain the decrease in the average size of nanowires, as well. The average domain size of the P3HT/$PC_{61}BM$ blend film fabricated from the P3HT NWs (Figure 3d) looks smaller and more uniform than that of the film fabricated by other methods such as thermal annealing (Figure 3c) and spontaneous aggregation in dipolar media as reported in the literature.[12]

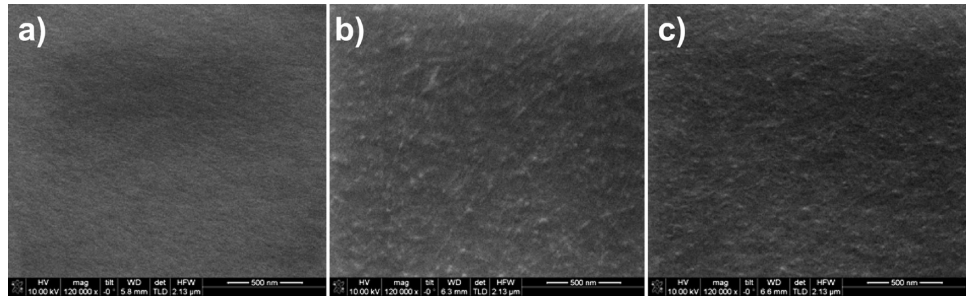

Figure 4. SEM images of P3HT/PCBM blend after thermals annealing: (a) 98% RR P3HT homogeneous solution, (b) 91% RR P3HT NW solution, and (c) 98% RR P3HT NW solution. Films were fabricated using spin-casting after adding PCBM to each of the P3HT solutions.

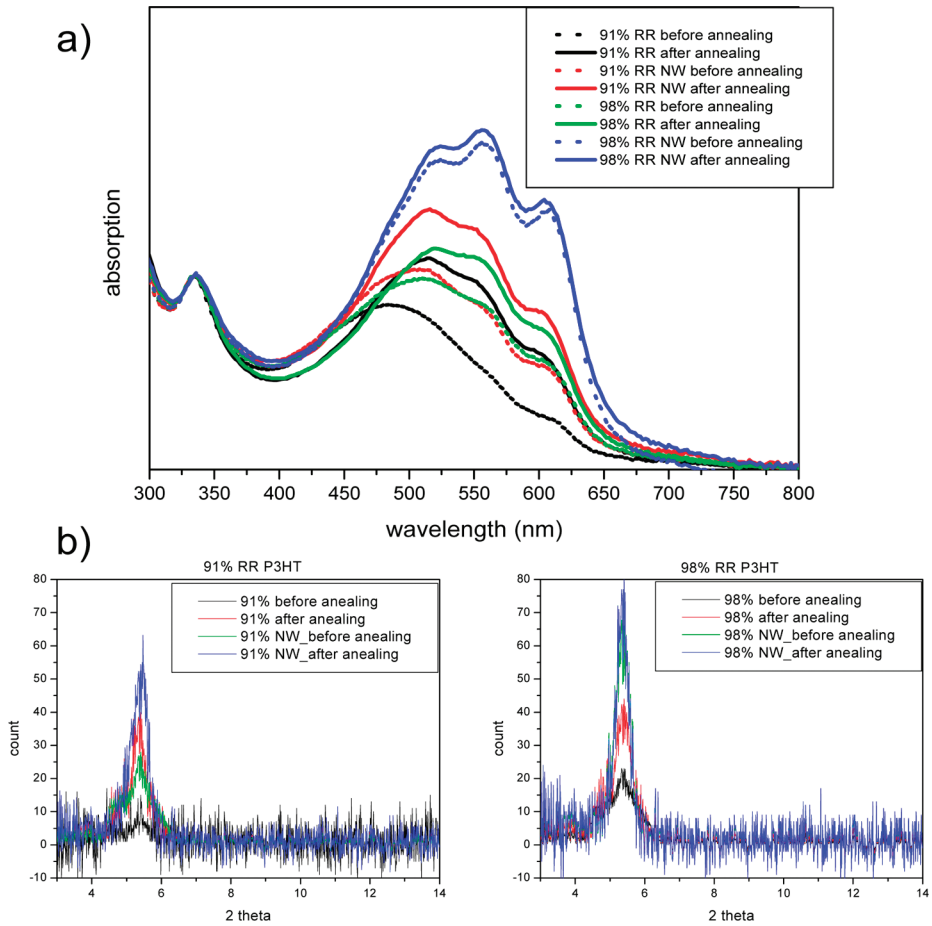

Figure 5. Effect of regioregularity on the crystalline packing of P3HT. (a) UV−vis spectra of spin-cast films of various P3HT/$PC_{61}BM$ systems and (b) their X-ray diffraction patterns.

Regioregularity Effect on Aggregation. We investigated the effect of the regioregularity of P3HT on the aggregation behavior by analyzing the absorption spectra of various P3HT/$PC_{61}BM$ systems. We examined spin-cast films of 91% RR P3HT/$PC_{61}BM$, 91% RR P3HT NW/$PC_{61}BM$, 98% RR P3HT/$PC_{61}BM$, and 98% RR P3HT NW/$PC_{61}BM$. Figure 5a clearly shows that the aggregation behavior of P3HT strongly depends on the regioregularity. The characteristic absorption peak of P3HT aggregates at 620 nm increased as the regioregularity of P3HT increased.[3] The absorption intensity of P3HT also increased with the regioregularity of P3HT. The films of preaggregated P3HT NW solutions, regardless of their regioregularity, show a higher absorption intensity than the films from the conventional P3HT/$PC_{61}BM$ solutions. The spin-cast film prepared from 91% RR P3HT solution shows a broad featureless absorption spectrum. As the film was thermally annealed, the absorption intensity increased with two distinct additional shoulders at around 550 and 600 nm, respectively. The resulting absorption spectrum is very similar to that of the spin-cast film of the 91% RR P3HT NW solution in terms of intensity and shape. As the film of the 91% RR P3HT NW solution was thermally annealed, the intensity increased further. These comparisons imply that the nanowire formation of P3HT in solution is a superior method to the thermal annealing of a spin-cast film from a homogeneous P3HT solution for making well-packed crystalline P3HT. The same trend was observed in 98% P3HT. However, the higher regioregularity provides much better packing of the polymer, as evidenced by the increased intensity of the respective spin-cast films relative to those of lower regioregularity. Compared to other cases, the very small increase of the absorption intensity of the 98% P3HT NW film after the thermal annealing implies that the crystallinity of the self-assembled 98% P3HT nanowire formed in solution is already maximized.

X-ray diffraction analysis on these films also confirms the same regioregularity effect on the crystalline packing of P3HT (Figure 5b). All samples showed only one strong diffraction peak at around 5.3°, and the peak intensity is dependent on the regioregularity of P3HT. The self-assembled P3HT NWs showed a stronger diffraction peak than the spin-cast film of the P3HT homogeneous solution having the same regioregularity. The diffraction peak intensity increased as the films were thermally annealed, indicating that thermal annealing induces better crystal packing of P3HT as we observed in the UV−vis analysis. A 98% regioregular P3HT NW

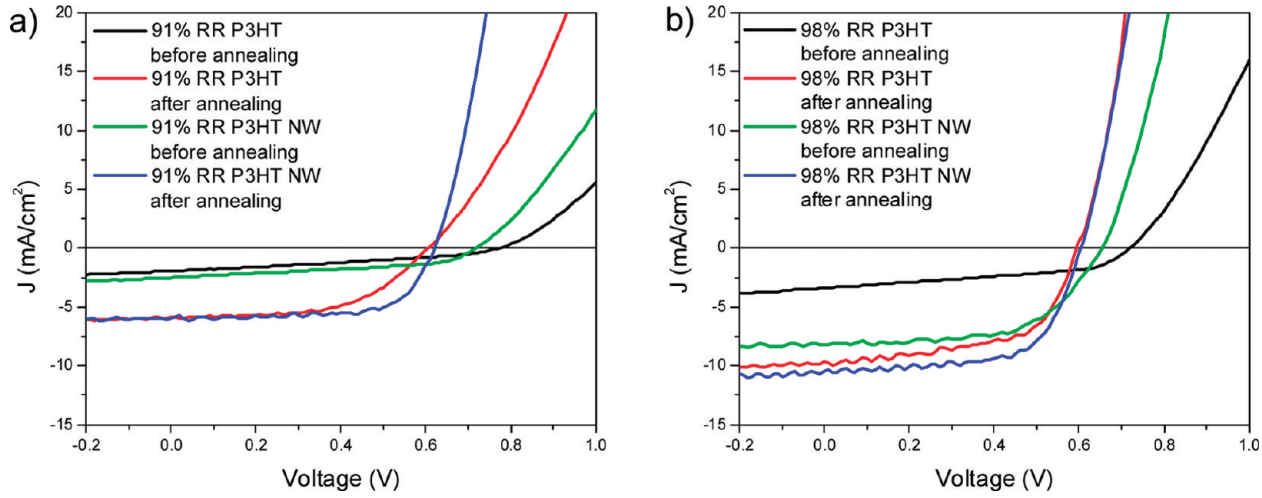

Figure 6. *J*−*V* curves of P3HT/$PC_{61}BM$ blend systems, (a) 91% RR and (b) 98% RR P3HT.

film has the highest crystallinity and was slightly increased by thermal annealing. This indicates that 98% regioregular P3HT formed highly ordered crystalline packing during the sonication-assisted self-assembly process due to the high regioregularity and freedom of movement in solution.

Application for Photovoltaic Devices. The *J*−*V* curves of the devices are shown in Figure 6, and the performance of the cells is summarized in Table 1. As one can clearly see from the results, the devices made of the sonication-assisted self-assembly of P3HT nanowires/$PC_{61}BM$ show the larger J_{sc}, FF, and PCE than the devices from the homogeneous solution of P3HT/$PC_{61}BM$ having the same regioregularity. While the shunt resistance of the devices is very similar to each other regardless of the fabrication method, the series resistance of the devices made of the sonication-assisted self-assembly of P3HT nanowires/$PC_{61}BM$ is much lower than that of the analogous devices from the homogeneous solution of P3HT/$PC_{61}BM$, demonstrating the efficiency of the sonication-assisted self-assembly of P3HT nanowires for solar cell fabrication. As the AFM investigation showed, sonication not only induces well-connected P3HT nanofibers but also likely helps $PC_{61}BM$ to be dispersed well on the nanofiber surfaces. This nanoscale phase separation will facilitate charge separation and transport, producing the larger fill factor (FF) and the enhanced short-circuit current observed from the devices made of the sonication-assisted self-assembled P3HT nanowires/$PC_{61}BM$.[18] In the same experimental conditions, devices fabricated with P3HT nanowires/$PC_{61}BM$ showed about 6−30% better FF than those from a conventional P3HT/$PC_{61}BM$ blend solution. Thermal annealing has a large effect on the device performance because thermal annealing can induce better P3HT packing, as we observed in the UV−vis study. Moreover, thermal annealing can fill the clefts between the nanowires with amorphous P3HT distributed around the P3HT nanowires, as evident in the AFM study. However, this effect was not significant for the already well-packed 98% RR P3HT NW/$PC_{61}BM$. The V_{oc} value of the well-packed P3HT/$PC_{61}BM$ decreased regardless of whether the thermal annealing or the sonication-assisted self-assembly was used. That is likely due to the strong intermolecular interaction between the donor P3HT and the acceptor $PC_{61}BM$.[19]

CONCLUSIONS

In summary, we have devised the sonication-assisted self-assembly of P3HT nanowires together with $PC_{61}BM$ in a cosolvent system containing acetonitrile, a polar solvent. The self-assembly behavior of P3HT depends not on the solubility power of the cosolvent system but on the solvent polarity. Also, the optimum volume ratio of acetonitrile to obtain a homogeneous P3HT NW suspension depends on the regioregularity of P3HT. There are several factors that affect the self-

TABLE 1. Device Performance of Photovoltaic Cells Made of Various P3HT/PC61BM Systems

	91% RR P3HT before thermal	91% RR P3HT after thermal	91% RR NW before thermal	91% RR NW after thermal	98% RR P3HT before thermal	98% RR P3HT after thermal	98% RR NW before thermal	98% RR NW after thermal
J_{sc} (mA/cm^{-2})	2.09	5.76	2.49	5.95	3.40	9.67	8.23	10.42
V_{oc} (V)	0.78	0.60	0.73	0.62	0.72	0.59	0.66	0.61
FF	0.34	0.58	0.45	0.65	0.46	0.60	0.58	0.64
PCE (%)	0.55	2.00	0.83	2.39	1.13	3.45	3.13	4.09
series resistance (Ω cm^2)	13.70	3.69	6.06	3.21	12.54	2.89	9.71	2.78
shunt resistance (Ω cm^2)	587	840	560	1460	412	804	998	1148

assembly of P3HT, such as ultrasonic irradiation, the illumination conditions, and the regioregularity of P3HT. The sonication-assisted self-assembly of P3HT together with $PC_{61}BM$ provided uniform nanowires having a diameter of 40−50 nm, which was confirmed by AFM analysis. As the regioregularity increased, more effective nanowire formation was observed, as evident in the UV−vis spectrophotometry and X-ray diffraction analysis. Thermal annealing enhanced further the packing of the nanofibers. Photovoltaic cells having a ITO/PEDOT-PSS/P3HT-$PC_{61}BM$/Al structure were fabricated from the self-assembled P3HT NW/$PC_{61}BM$ and a homogeneous P3HT/$PC_{61}BM$ solution, and their device performance was compared and analyzed in connection with the AFM, UV−vis, and XRD results. Devices made of the self-assembled P3HT nanowires/$PC_{61}BM$ showed better J_{sc}, series resistance, fill factor, and power conversion efficiency. Thermally annealed photovoltaic cells having the self-assembled 98% regioregular P3HT nanowires/$PC_{61}BM$ by the sonication-assisted self-assembly achieved 4.09% power conversion efficiency. The devised sonication-assisted self-assembly method of P3HT is a promising tool to prepare well-defined P3HT nanowires together with other additives and is useful for various organic electronic applications and suitable for roll-to-roll mass production[20,21] because it can obtain fully assembled P3HT without a long-time annealing process.

METHODS

Materials. $PC_{61}BM$ was purchased from American Dye source. The 91% regioregular P3HT was purchased from Rieke Metals and used without further purification. The 98% regioregular P3HT was synthesized by means of GRIM polymerization, as reported previously.[22] Obtained polymer was purified using precipitation into methanol and Soxhlet extraction. After removing oligomers by the precipitation and Soxhlet extraction, the polymer was further purified by means of column purification through Celite and magnesium silicate. Regioregularity of the polymers was verified with ^{1}H NMR (M_n = 55 000, M_w = 88 000, PDI = 1.6).

Nanowire Suspension and Blend Solution. After dissolving 10 mg of P3HT in a chlorobenzene/acetonitrile cosolvent system (0.7 mL/0.07 mL for 91% RR P3HT and 1.0 mL/0.07 mL for 98% RR P3HT), the obtained orange solution was treated with ultrasonication at room temperature for 2 min. The solution was kept under ambient condition for 2 h to allow P3HT crystallization in the solution state. Ten milligrams of $PC_{61}BM$ was dissolved in the same cosolvent composition (0.3 mL/0.03 mL for 91% RR P3HT and 0.3 mL/0.2 mL for 98% RR P3HT) and added to the P3HT nanowire suspension under ultrasonication. The resulting blend solution was used for AFM, UV−vis, XRD, and device fabrication after applying further ultrasonication for 2 min to enhance the penetration of $PC_{61}BM$ homogeneously into P3HT nanowires. In the case of a blend solution for the thermally annealed film, 10 mg of P3HT and PCBM was dissolved in 1.0 mL of chlorobenzene and was used for the same characterization.

Device Fabrication and Characterization. ITO-coated glasses were cleaned with acetone and IPA followed by UV ozone treatment for 5 min. PEDOT:PSS (Baytron PH 500) was spin-cast on the substrate and baked at 150 °C for 15 min. Different P3HT/$PC_{61}BM$ blend solutions with and without P3HT nanowire were prepared and spin-cast at 700 rpm for 30 s. To dry the solvent completely, the casted films were additionally spun at 3000 rpm for 2 min. In the case of thermally annealed samples, they were annealed for 15 min at 150 °C. Final devices were fabricated by depositing a 1 nm thick LiF and a 100 nm Al layer (9.62 mm^2, circle shape) sequentially under 5×10^{-7} Torr. We used the island-type electrode geometry to prevent the additional charge collection observed from the crossbar-type device configuration.[23] All devices were characterized under ambient conditions, and the typical illumination intensity was 100 mW/cm^2 (AM 1.5G Oriel solar simulator).

Acknowledgment. This work was supported by Department of Energy EFRC Grant (DE-SC0000957) and Michigan Memorial Phoenix Energy Institute (MMPEI).

Supporting Information Available: Supporting aggregation behaviors, and a video of aggregation development by ultrasonication. This material is available free of charge *via* the Internet at http://pubs.acs.org.

REFERENCES AND NOTES

1. Lee, K.; Kim, J. Y.; Coates, N. E.; Moses, D.; Nguyen, T.-Q.; Dante, M.; Heeger, J. Efficient Tandem Polymer Solar Cells Fabricated by All-Solution Processing. *Science* **2007**, *317*, 222.
2. Yang, C.; Ma, W.; Gong, X.; Lee, K.; Heeger, A. J. Thermally Stable, Efficient Polymer Solar Cells with Nanoscale Control of the Interpenetrating Network Morphology. *Adv. Funct. Mater.* **2005**, *15*, 1617.
3. Li, G.; Shrotriya, V.; Huang, J.; Yao, Y.; Moriarty, T.; Emery, K.; Yang, Y. High-Efficiency Solution Processable Polymer Photovoltaic Cells by Self-Organization of Polymer Blends. *Nat. Mater.* **2005**, *4*, 864.
4. Kim, Y.; Cook, S.; Tuladhar, S. M.; Choulis, S. A.; Nelsonm, J.; Durrant, J. R.; Bradley, D. C.; Giles, M.; Mcculloch, I.; Ham, C.-S.; Ree, M. A Strong Regioregularity Effect in Self-Organizing Conjugated Polymer Films and High-Efficiency Polythiophene:Fullerene Solar Cells. *Nat. Mater.* **2006**, *5*, 197.
5. Hoth, C. N.; Schilinsky, P.; Choulis, S. A.; Brabec, C. J. Printing Highly Efficient Organic Solar Cells. *Nano Lett.* **2008**, *8*, 2806.
6. Peet, J.; Kim, J. Y.; Coates, N. E.; Ma, W. L.; Moses, D.; Heeger, A. J.; Bazan, G. C. Efficiency Enhancement in Low-Bandgap Polymer Solar Cells by Processing with Alkane Dithiols. *Nat. Mater.* **2007**, *6*, 497.
7. Berson, S.; Bettignies, R.; Bailly, S.; Guillerez, S. Poly(3-hexylthiophene) Fibers for Photovoltaic Applications. *Adv. Funct. Mater.* **2007**, *17*, 1377.
8. Oosterbaan, W. D.; Vrindts, V.; Berson, S,; Guillerez, S.; Douhéret, O.; Ruttens, B.; D'Haen, J.; Adriaensens, P.; Manca, J.; Lutsenc, L.; Vanderzande, D. Efficient formation, Isolation and Characterization of Poly(3-alkylthiophene) Nanofibres: Probing Order as a Function of Side-Chain Length. *J. Mater. Chem.* **2009**, *19*, 5424–5435.
9. Liu, J.; Arif, M.; Zou, J.; Khondaker, S. I.; Zhai, L. Controlling Poly(3-hexylthiophene) Crystal Dimension: Nanowhiskers and Nanoribbons. *Macromolecules* **2009**, *42*, 9390.
10. Samitsu, S.; Shimomura, T.; Heike, S.; Hashizume, T.; Ito, K. Effective Production of Poly(3-alkylthiophene) Nanofibers by Means of Whisker Method Using Anisole Solvent: Structural, Optical, and Electrical Properties. *Macromolecules* **2008**, *41*, 8000–8010.
11. Zhang, F.; Jespersen, K. G.; Björström, C.; Svensson, M.; Andersson, M. R.; Sundström, V.; Magnusson, K.; Moons, E.; Yartsev, A.; Inganäs, O. Influence of Solvent Mixing on the Morphology and Performance of Solar Cells Based on Polyfluorene Copolymer/Fullerene Blends. *Adv. Funct. Mater.* **2006**, *16*, 667.
12. Moulé, A. J.; Meerholz, K. Controlling Morphology in Polymer-Fullerene Mixtures. *Adv. Mater.* **2008**, *20*, 240.

13. Horn, D.; Rieger, J. Organic Nanoparticles in the Aqueous Phase—Theory, Experiment, and Use. *Angew. Chem., Int. Ed.* **2001**, *40*, 4330.
14. Bucar, D. K.; MacGillivray, L. R. Preparation and Reactivity of Nanocrystalline Cocrystals Formed *via* Sonocrystallization. *J. Am. Chem. Soc.* **2007**, *129*, 32.
15. Hasobe, T.; Oki, H.; Sandanayaka, A. S. D.; Murata, H. Sonication-Assisted Supramolecular Nanorods of *meso*-Diaryl-Substituted Porphyrins. *Chem. Commun.* **2008**, 724.
16. The information of polarity index on several solvents was taken from www.chemical-ecology.net/java/solvents.htm.
17. Sluch, M. I.; Godt, A.; Bunz, U. H. F.; Berg, M. A. Excited-State Dynamics of Oligo(*p*-phenylene ethynylene): Quadratic Coupling and Torsional Motions. *J. Am. Chem. Soc.* **2001**, *123*, 6447.
18. Kim, M.-S.; Kim, B.-G.; Kim, J. The Effective Variables to Control the Fill Factor of Organic Photovoltaic Cells. *ACS Applied Materials & Interfaces* **2009**, *1*, 1264.
19. Perez, M. D.; Borek, C.; Forrest, S. R.; Thompson, M. E. Molecular and Morphological Influences on the Open Circuit Voltages of Organic Photovoltaic Devices. *J. Am. Chem. Soc.* **2009**, *131*, 9281.
20. Krebs, F. C. Fabrication and Processing of Polymer Solar Cells: A Review of Printing and Coating Techniques. *Sol. Energy Mater. Sol. Cells* **2009**, *93*, 394.
21. Krebs, F. C.; Gevorgyan, S. A.; Alstrup, J. A Roll-to-Roll Process to Flexible Polymer Solar Cells: Model Studies, Manufacture and Operational Stability Studies. *J. Mater. Chem.* **2009**, *19*, 5442.
22. Loewe, R. S.; Ewbank, P. C.; Liu, J.; Zhai, L.; McCullough, R. D. Regioregular, Head-to-Tail Coupled Poly(3-alkylthiophenes) Made Easy by the GRIM Method: Investigation of the Reaction and the Origin of Regioselectivity. *Macromolecules* **2001**, *34*, 4324–4333.
23. Kim, M.-S.; Kang, M.-G.; Guo, L. J.; Kim, J. Choice of Electrode Geometry for Accurate Measurement of Organic Photovoltaic Cell Performance. *Appl Phys. Lett.* **2008**, *92*, 133301.